The Tibetan Ozone Low and Its Long-Term Variation During 1979–2010

ZHOU Libo* (周立波), ZOU Han (邹 捍), MA Shupo (马舒坡), and LI Peng (李 鹏)

LAPC & LAOR, Institute of Atmospheric Physics, Chinese Academy of Sciences, Beijing 100029

(Received May 30, 2012; in final form October 26, 2012)

ABSTRACT

A Tibetan ozone low was found in the 1990s after the Antarctic ozone hole. Whether this ozone low has been recovering from the beginning of the 2000s following the global ozone recovery is an intriguing topic. With the most recent merged TOMS/SBUV (Total Ozone Mapping Spectrometer/Solar Backscatter Ultra Violet) ozone data, the Tibetan ozone low and its long-term variation during 1979–2010 are analyzed using a statistical regression model that includes the seasonal cycle, solar cycle, quasi-biennial oscillation (QBO), ENSO signal, and trends. The results show that the Tibetan ozone low maintains and may become more severe on average during 1979–2010, compared with its mean state in the periods before 2000, possibly caused by the stronger downward trend of total ozone concentration over the Tibet. Compared with the ozone variation over the non-Tibetan region along the same latitudes, the Tibetan ozone has a larger downward trend during 1979–2010, with a maximum value of –0.40±0.10 DU yr^{-1} in January, which suggests the strengthening of the Tibetan ozone low in contrast to the recovery of global ozone. Regression analyses show that the QBO signal plays an important role in determining the total ozone variation over the Tibet. In addition, the long-term ozone variation over the Tibetan region is largely affected by the thermal-dynamical proxies such as the lower stratospheric temperature, with its contribution reaching around 10% of the total ozone change, which is greatly different from that over the non-Tibetan region.

Key words: Tibetan ozone low, long-term ozone variation, dynamical proxies

Citation: Zhou Libo, Zou Han, Ma Shupo, et al., 2013: The Tibetan ozone low and its long-term variation during 1979–2010. *Acta Meteor. Sinica*, **27**(1), 75–86, doi: 10.1007/s13351-013-0108-9.

1. Introduction

As one important greenhouse gas, the atmospheric ozone has great influences on the global climate and environmental system. In the 1980s, a strong ozone depletion called “ozone hole” was found over the Antarctic region (e.g., Farman et al., 1985), and thereafter the global ozone depletion has been well studied (e.g., Manney et al., 1994; Bodeker et al., 2001; Fioletov et al., 2002; WMO, 2003, 2007). In the 1990s, an ozone low called “ozone valley” over the Tibetan region was also revealed (e.g., Zhou and Luo, 1994), following the strong Antarctic ozone depletion. From then on, many studies have been conducted to investigate the Tibetan ozone low and its formation and variation mechanisms. For example, Zhou et al. (1995) pointed out that the Tibetan ozone valley can be characterized with the monthly mean total ozone over the Tibetan region being around 20–30 DU lower than that over the other areas along the Tibetan latitudes belt from June to September, based on the Nimbus-7 TOMS (Total Ozone Mapping Spectrometer) data during 1979–1991. They argued that the Tibetan ozone low is mainly caused by the upward motions due to the Tibetan heating, which can carry the poor-ozone air from the troposphere into the lower stratosphere and result in the low total column ozone. Using the same dataset, Zou (1996) also found the Tibetan ozone valley in spring and summer, and suggested a close relationship between the Tibetan ozone deficiency and the local heating. Based on analyses of the ozonesonde data over Lhasa from June to October

Supported by the National Basic Research and Development (973) Program of China (2009CB421403), State Oceanic Administration Public Science and Technology Research Fund (201005017-5), China Meteorological Administration Special Public Welfare Research Fund (GYHY201106018), and State Oceanic Administration Polar Environment Investigation and Assessment Project (CHINARE2012-04-04 and CHINARE2012-02-03).

*Corresponding author: zhoulibo@mail.iap.ac.cn.

1998, Zheng et al. (2000) confirmed existence of the ozone valley over the Tibet. The dominant dynamical mechanism for the Tibetan ozone valley was further proved by later observational studies and model simulations (Zou and Gao, 1997; Bian et al., 1997; Fu et al., 1997; Cong et al., 2001; Liu et al., 2003; Ye and Xu, 2003; Xu and Chen, 2006; Tian et al., 2008; Guo et al., 2012).

Besides studies of the Tibetan ozone low and its mechanism, there are also some studies on the long-term ozone variation over the Tibetan region. For example, Zou (1996) studied the long-term ozone trends over the Tibet using Nimbus-7 TOMS data during 1979–1991. His results showed that there existed a strong downward trend of ozone concentration over the Tibet, with the average value of –0.79±0.82 DU yr^{-1} and monthly trends ranging from –0.17 to –1.79 DU yr^{-1}. With the same data, Zou et al. (2000, 2001) also analyzed the effects of the quasi-biennial oscillation (QBO) and the El Niño and Southern Oscillation (ENSO) signal in the long-term ozone variation over the Tibet. The ozone QBO was detected over the Tibet, with an amplitude of 8 DU and a period of 29 months. The ENSO-related ozone variation has smaller amplitudes compared with that over the Southern Hemisphere (Zou et al., 2000, 2001). Liu and Li (2001) also found the decreasing trends of ozone concentration over the Tibetan Plateau (TP) from 1979 to 1992, with the maximum decreasing rate of –0.336% yr^{-1}. Zhou and Zhang (2005) presented the decadal ozone trends over the TP using the merged ozone data from 1979 to 2002 and found that the downward trends are closely related to the long-term changes of temperature and geopotential height.

It is known that the ozone trends rely strongly on the data length (e.g., Guillas et al., 2004). For example, Austin et al. (2008) pointed out that the ozone data should include at least two solar cycles (around 22 yr) for assessing the long-term ozone trends more accurately. With addition of several years of the 2000s, the reduction of ozone depletion rates in midlatitudes of the Northern Hemisphere (NH) was identified (e.g., Newchurch et al., 2003; Reinsel et al., 2002, 2005; WMO, 2003, 2007).

As an important geographic feature in the NH midlatitudes, the TP plays an essential role in the global ozone variation through thermal and dynamical forcing (e.g., Ye and Xu, 2003; Randel and Park, 2006; Tian et al., 2008). Most previous studies demonstrated the severe Tibetan ozone low and its strong strengthening trends, but with rather short periods (e.g., Zou, 1996; Zou et al., 2000, 2001; Liu and Li, 2001). Studies showed that the global ozone has entered a recovery period since the 2000s (WMO, 2007). Under the background of global ozone recovery, does the severe ozone low over the Tibetan region even exist or not? Does the strong declining trend of ozone continue over the Tibet?

In the present study, with the most recent merged ozone data from 1979 to 2010, the local ozone deficiency over the TP is recalculated, and the long-term ozone trends are retrieved from a statistical regression model, in comparison with the results of previous studies. In addition, the long-term ozone variation and the possible contributing climate factors such as solar cycle, QBO, and ENSO are quantified in this paper. The adopted data and methodology are described in Section 2. The distribution and variation of the Tibetan ozone low are presented in Section 3. The long-term ozone variation and contributions from climate factors are analyzed in Section 4. Conclusions are given in Section 5.

2. Data and methodology

The ozone data used in this study are TOMS/SBUV (Solar Backscatter UltraViolet) merged total ozone data (http://code916.gsfc.nasa.gov/Data_services/merged/data/toms_ sbuv_ v8_ mod_v3_70-10_5x10_rev5.txt) from 1979 to 2010. The monthly mean temperature, geopotential height, and zonal wind are from the ECMWF interim dataset available at http://data-portal.ecmwf.int/data/d/interim_moda/. An area-weighted (cos(latitude)) mean is applied to two regions, i.e., 25°–40°N, 75°–105°E for the Tibetan region, and 25°–40°N latitude zone without 75°–105°E for the non-Tibetan region. The zonal ozone deviation is obtained by subtracting the zonal mean from the area-weighted mean.

A statistical regression equation is used in this study to derive the seasonal ozone trends from the time series of ozone data. In addition, the variables such as solar cycle, QBO, and ENSO signals are also included in the regression equation to exclude their effects on ozone trends and to assess their contributions to the ozone variation. The regression equation is similar to that of Ziemke et al. (1997) and Zhou et al. (2003), which has the following form:

$$\mathrm{TO_3} = \alpha + \beta t + \gamma \mathrm{solar}(t) + \delta \mathrm{QBO}_{30}(t-\lambda) + \eta \mathrm{ENSO}(t) + R(t), \tag{1}$$

where α, β, γ, ε, δ, and η are time-dependent regression coefficients given by a constant plus 12-, 6-, and 4-mon cosine and sine harmonic series. The coefficient α denotes seasonal variability, β is the trend term, and $\gamma\mathrm{solar}(t)$, $\delta\mathrm{QBO}_{30}(t-\lambda)$, and $\eta\mathrm{ENSO}(t)$ represent the solar, QBO, and ENSO proxies-associated regression fits, respectively. The time series of ozone residuals is represented by $R(t)$, denoting the regression error. The solar index is the standardized 10.7-cm solar radio flux, the QBO index is the standardized 30-hPa zonal winds, and the ENSO signal is obtained from the difference between Tahiti and Darwin-normalized sea level pressure. The time series of the QBO signal are selected as in Randel et al. (1995), adjusting the phase lag λ to maximize the cross correlation with the QBO signal in equatorial TOMS ozone and then using the same lag value for other latitudes. The phase lag value here is four months.

3. The Tibetan ozone low

To characterize the Tibetan ozone low, the zonal ozone deviation obtained by subtracting the zonal mean from the total ozone is calculated over the Tibetan region (25°–40°N, 75°–105°E) in Fig. 1. It is seen that the local ozone deficiency (represented by zonal ozone deviation) over the Tibetan is the strongest in May (–24.0 DU) and the weakest in January (–1.7 DU) during 1979–2010. This seasonal cycle of ozone deficiency is quite similar to that calculated during 1979–1991 using TOMS Nimbus-7 dataset in Zou (1996), but with a little amplitude difference, which could be related to the usage of different datasets. To investigate variation of the Tibetan ozone low during the last decade when the global ozone recovery occurred, the Tibetan ozone deficiency during 2000–2010 is also calculated and plotted in Fig. 1, in comparison with that during 1979–1999. During 2000–2010, the Tibetan ozone deficiency is not weakened; it is even a little strengthened compared with those in the other two periods, which is in contrast to the global ozone recovery. This suggests the existence and the even more severity of the ozone low over the Tibetan region during this period.

Figure 2 further illustrates the horizontal distribution of zonal ozone deviation in May when the most severe ozone deficiency occurred over the Tibet during periods of 1979–2010, 1979–1999, and 2000–2010. During 1979–2010, a strong ozone low occurred over the Tibetan region, with the averaged ozone concentration value lower than –20 DU and the minimum of –35.4 DU centered at 35°N, 85°E. Similar distributions of ozone deficiency are also found during the other two periods, with strong ozone deficiencies appearing over the Tibetan region. In comparison, the ozone deficiency is the most severe during 2000–2010, with values lower than –30 DU covering most of the Tibetan region, and the two minima of –36.6 and –36.1 DU centered at 37.5°N, 75°E and 32.5°N, 85°E.

Therefore, the Tibetan ozone low still exists during 1979–2010, with the lowest ozone concentration in May. Contrary to the global ozone recovery in the beginning of the 21st century, the Tibetan ozone deficiency may even become a little strengthened during

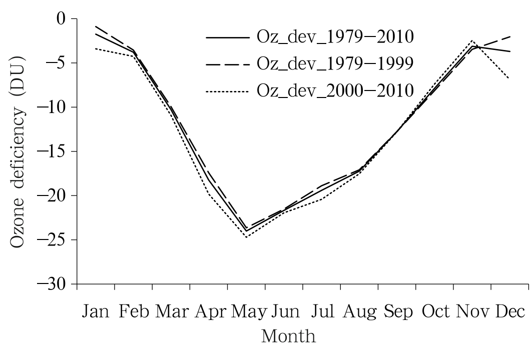

Fig. 1. Seasonal cycle of local ozone deficiency over the Tibetan region, averaged for 1979–2010 (solid curve), 1979–1999 (dashed curve), and 2000–2010 (dotted curve), respectively.

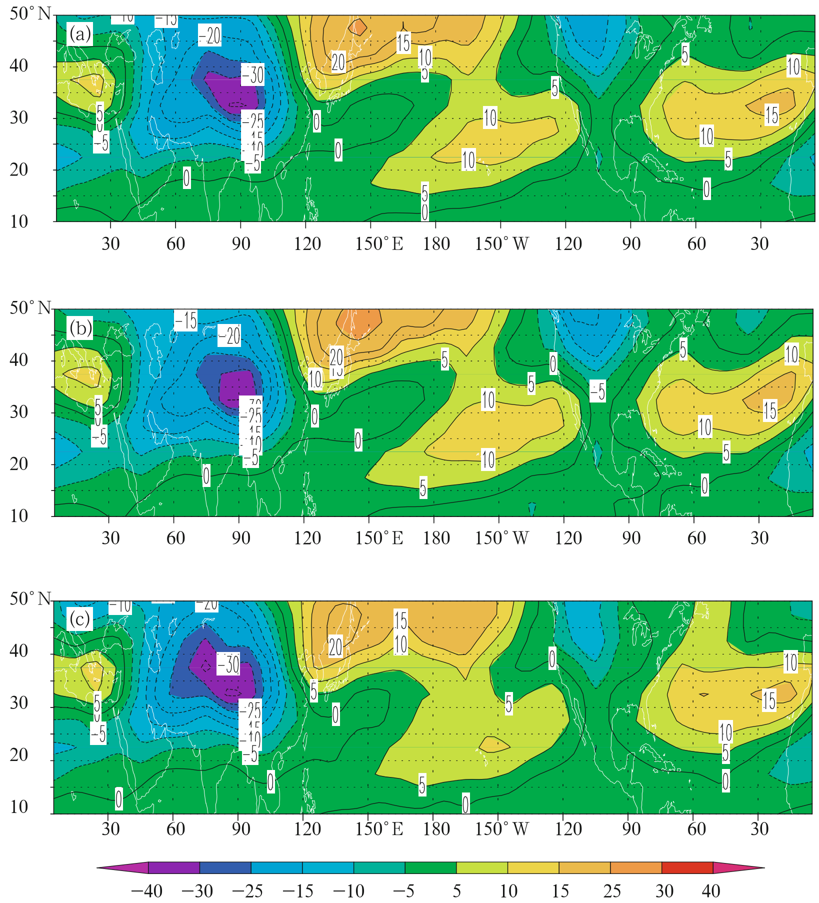

Fig. 2. Horizontal distributions of ozone deficiency in May during the periods of (a) 1979–2010, (b) 1979–1999, and (c) 2000–2010.

the last decade, which could be related to the slower rate of ozone increase over the Tibetan region than over the same latitude belt, and this will be discussed in the next section.

4. Long-term variation of the Tibetan ozone low

The above analysis shows that strong ozone deficiency exists during 1979–2010 and may be more intensified during the most recent decade. To investigate the possible reason, the long-term ozone variation over the Tibetan region is analyzed in the following, especially the ozone trends. In addition, the possible contributions to the long-term ozone variation over the Tibetan region of different climate factors are also discussed, in comparison with those over the non-Tibetan region.

4.1 Long-term ozone variation and its regression fits

Derivation of trends in ozone over time relies on the statistical regression models (WMO, 2003), which should consider the seasonal variation of ozone trends and influences from climate factors. In this study, Eq. (1) given in Section 2 of this paper is applied to the time series of total ozone, following WMO (2003), Ziemke et al. (1997), and Zhou et al. (2003), in which the solar cycle, QBO, ENSO signals are included to improve the estimates of ozone trends. In addition, the contributions of these climate factors to the long-term ozone variation are also discussed.

By applying Eq. (1) to the long-term total ozone variation over the Tibetan latitudes belt, the overall ozone fits and corresponding season-, trend-, solar-, QBO- and ENSO-associated fits are obtained. As an

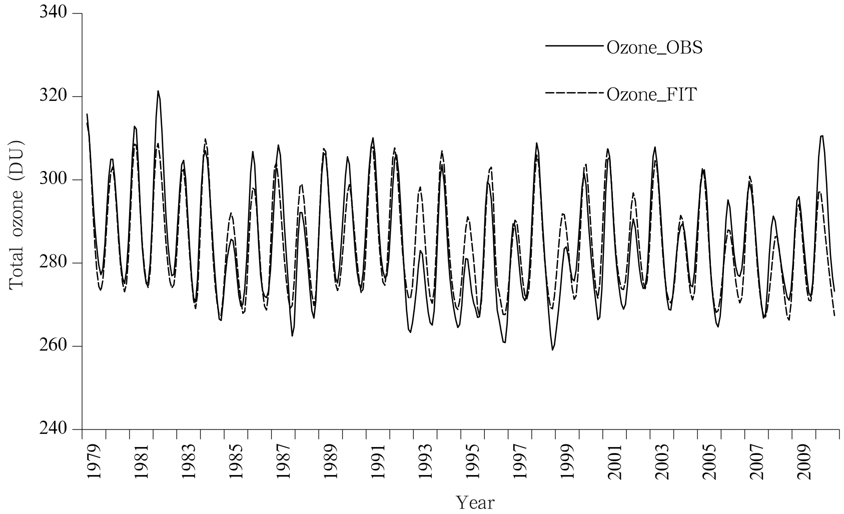

Fig. 3. Long-term variation of observed total ozone over the Tibet (solid curve) and its regression fit derived from the statistical regression (dashed curve) during 1979–2010.

example, Fig. 3 shows the long-term variation of observed total ozone over the TP (solid curve) and its regression fit. The two curves agree well, especially between their phase variations, despite of some magnitude differences in the extremely low ozone years such as 1987, 1993, and 1998. In fact, we also compared the longitudinal distribution and seasonal variation of total ozone and their regression fits (figures omitted). The regressed ozone fits retrieved similar results as the observations, which means that the total ozone variation can be described by the seasonal variability, trends, solar, QBO, and ENSO-associated regression fits.

4.2 Ozone trends

Figure 4a shows the longitudinal distribution of ozone trends, retrieved from Eq. (1), over the Tibetan latitudes belt from January to December. During 1979–2010, the total ozone strongly decreases (large negative trends) in winter and spring, and weakly increases in summer and autumn. The strongest decreasing trends occur over the central Pacific (around 150°–200°E) and the Tibetan region (70°–100°E), with the center value lower than –0.5 DU yr^{-1}. Figure 4b presents the seasonal variations of ozone trends over the Tibetan and non-Tibetan regions, with standard errors plotted. The downward ozone trends decrease from winter to summer, with the strongest downward trend occurring in the winter-spring seasons over both the Tibetan and non-Tibetan regions. The largest downward trend of total ozone is –0.40±0.10 DU yr^{-1}

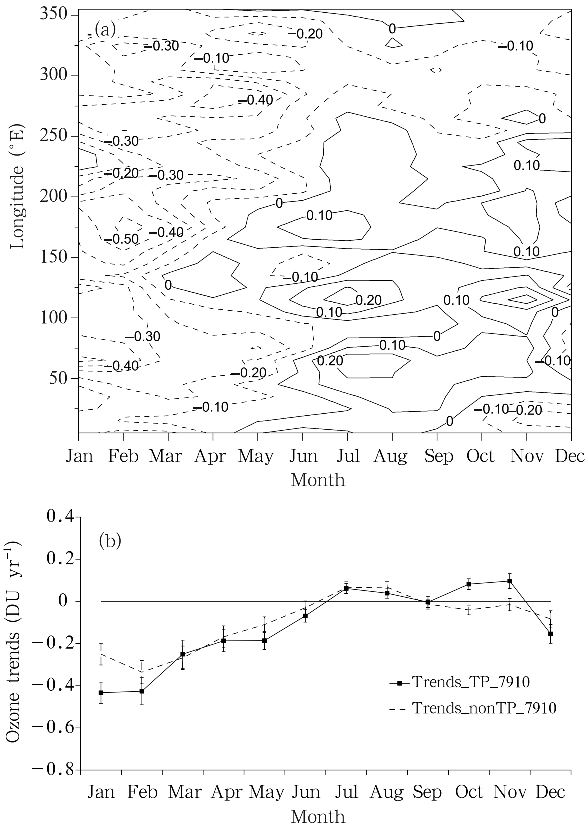

Fig. 4. Seasonal variations of ozone trends over (a) the Tibetan latitudes belt and (b) the Tibetan (solid curve) and non-Tibetan (dotted curve) regions with standard errors plotted.

in January over the Tibetan region and –0.29±0.09 DU yr^{-1} in February over the non-Tibetan region. Compared with the non-Tibetan region, the winter-spring ozone downward trends over the Tibetan region are larger, which results in the strengthening of local ozone deficiency in Figs. 1 and 2.

Figure 5 further presents the ozone trends over the Tibetan and non-Tibetan regions during periods of 1979–1999 and 2000–2010. Similar to that during 1979–2010, the downward trends of total ozone persists during 1979–1999, with seasonal trends ranging from –0.17±0.11 to –1.05±0.22 DU yr^{-1} for the Tibetan region and from 0.08±0.12 to –0.75±0.18 DU yr^{-1} for the non-Tibetan region. The downward ozone trend is a little stronger over the Tibetan than the non-Tibetan region. During 2000–2010, the ozone has an increasing trend for most of the year, but the trend values are almost insignificant at the 2σ level. The increasing ozone trend over the Tibetan region is a little smaller than those over the non-Tibetan region.

In general, compared with that over the non-Tibetan region, the total ozone over the Tibetan region has a stronger downward trend during 1979–1999 and a weaker increasing trend during 2000–2010, which causes the larger downward trends during 1979–2010 and the more intensified local ozone deficiency in Figs. 1 and 2.

4.3 Contributing climate factors

After removing the seasonal variability from the total ozone variation, there is an ozone anomaly, which should include the variations associated with trends, solar cycle, QBO, ENSO signals, etc. To quantitatively study the contributions of each climate factor to the long-term ozone variation over the Tibetan region, the ozone anomaly, together with the trends, solar cycle, QBO, and ENSO-associated fits, is given in Fig. 6a. It is clearly seen that these fits explain most of the ozone anomaly, in which the trends, solar cycle, and ENSO-associated regression fits indicate small amplitudes, ranging from 4% to 6% in total ozone, while the QBO-associated regression fit indicates a 10% contribution to the total ozone. Compared with the affecting factors to the Tibetan ozone variation, the trends, solar cycle, and ENSO-associated regression fits for the non-Tibetan region have smaller amplitudes, ranging from 3% to 4% in total ozone, while the QBO-associated regression fit contributes to 9% of the total ozone (see Fig. 6b). Figure 7 presents the regression errors between the ozone anomaly and total regression fits by the above climate factors. Large regression errors occur in 1982, 1987, 1993, 1999, and 2010. In addition, the regression error over the Tibetan region is much larger than that over the non-Tibetan region, which may suggest other potential factors affecting the long-term ozone variation over the Tibetan region.

Since the ozone QBO has a great contribution to the long-term ozone variation over both the Tibetan and non-Tibetan regions, the time-longitude section of the ozone QBO coefficients and its zonal mean

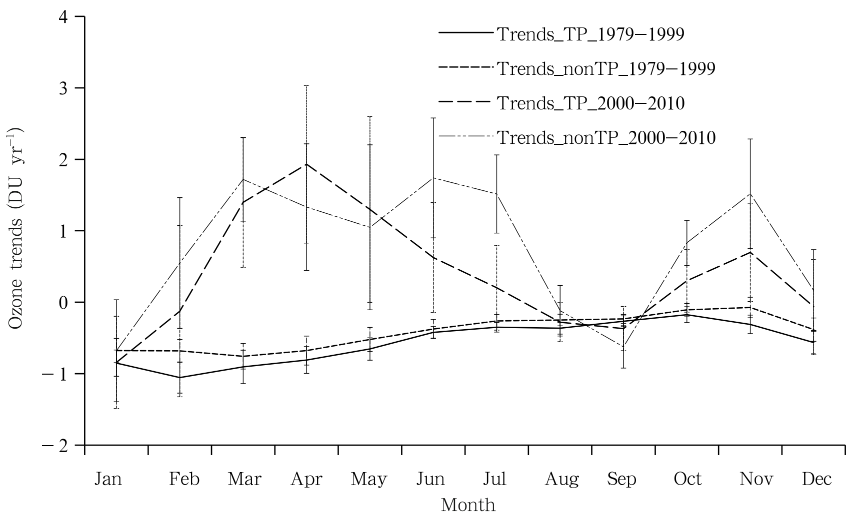

Fig. 5. Seasonal variations of ozone trends over the Tibetan and non-Tibetan regions during 1979–1999 and 2000–2010.

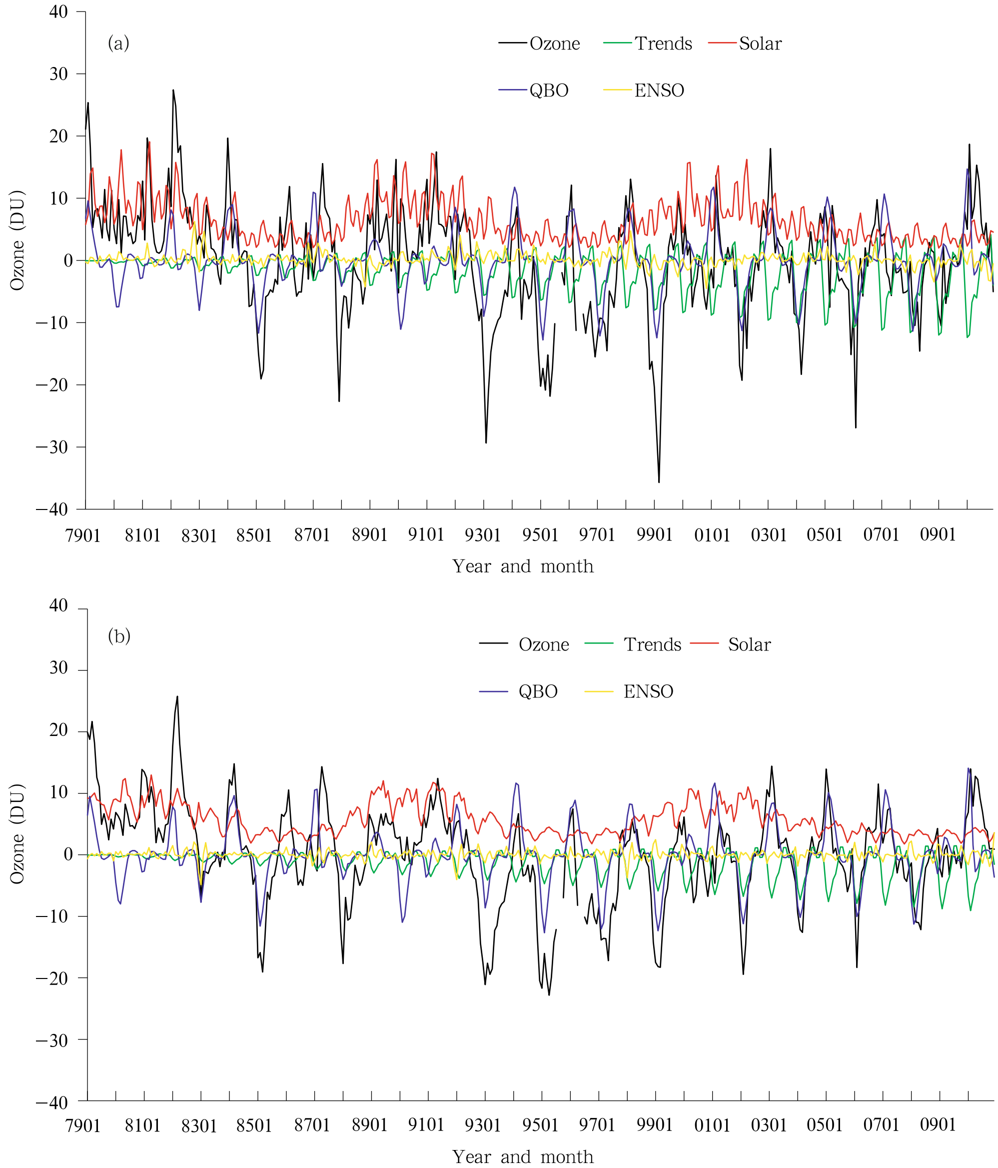

Fig. 6. Long-term variations of ozone anomaly, trends, solar cycle, QBO, and ENSO-associated fits over (a) the Tibetan region and (b) the non-Tibetan region.

obtained from Eq. (1) are shown in Figs. 8a and 8b. Strong negative values are found over the Tibetan latitudes in the winter-spring seasons, with the zonal mean minimum of -7.7 ± 0.9 DU per 10 m s^{-1} in February, which is anti-phase to the ozone QBO over the equator and the QBO index (e.g., Randel and Cobb, 1994). Although the QBO signal in total ozone over the subtropics is almost zonally symmetric (Baldwin et al., 2001; Zhou et al., 2003), the ozone QBO over the Tibetan latitudes belt occurs with some longitudinal variation, with the large negative values less than -8.0 DU per 10 m s^{-1} observed over the longitudes of 50°–80°E and 230°–250°E. It should be noticed that the QBO signals in total ozone have smaller positive values less than 2.0 DU per 10 m s^{-1} during the summer-autumn seasons, but not significant at the 2σ level, which is also shown in Fig. 8b.

4.4 Local thermal-dynamical proxies

Ziemke et al. (1997) pointed out that the dynamical proxies, e.g., temperature and geopotential height, could have great influences on the long-term ozone

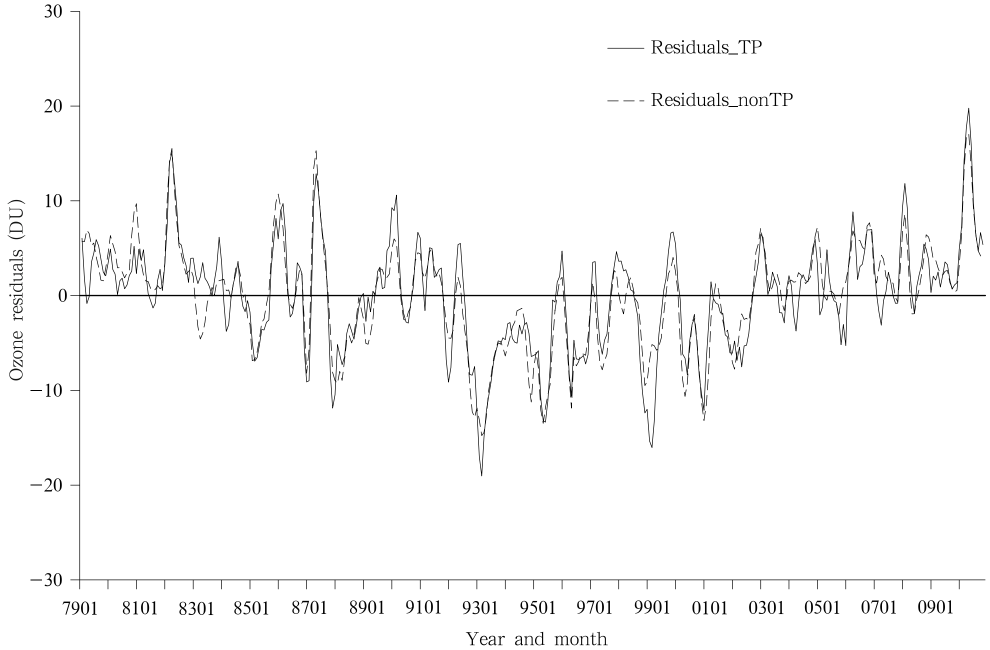

Fig. 7. Ozone residuals retrieved from Eq. (1) over the Tibetan (solid curve) and non-Tibetan regions (dashed curve).

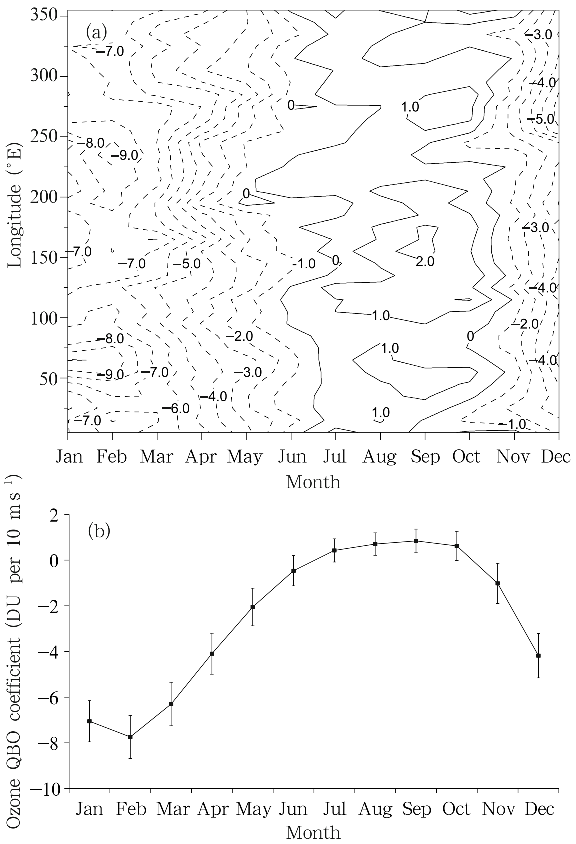

Fig. 8. Longitudinal distribution of ozone QBO coefficient from January to December over (a) the Tibetan latitudes belt and (b) its zonal mean with the standard errors also plotted.

variation and effectively reduce the regression errors. From the above, the traditional climate factors such as solar cycle, QBO, and ENSO cannot explain the entire long-term ozone variation, in particular over the Tibetan region. Figure 9 gives the longitudinal distribution of regression errors (residuals term $R(t)$ in Eq. (1)) over the Tibetan latitudes belt. The shadings denote areas with absolute residuals larger than 10 DU during 1979–2010. It is displayed that the regression ozone fits are much smaller than the observed ozone values over all the longitudes during 1993–2002. Therefore, it is necessary to investigate the reason for such a large difference. In this study, temperature was selected as a typical thermal-dynamical proxy. In fact, we also calculated geopotential height and wind speed and found similar results.

Figure 10 presents the correlation coefficients between the total ozone and temperature over the Tibetan latitudes belt during 1979–2010. Before the correlation analysis, the total ozone and temperature data are deseasonalized and linearly detrended, following the methods of Ziemke et al. (1997). The correlation coefficient shows positive values in the lower stratosphere, maximizing at around 50 hPa, and negative values in the middle and upper troposphere, maximizing around 300 hPa, and the zero value over the

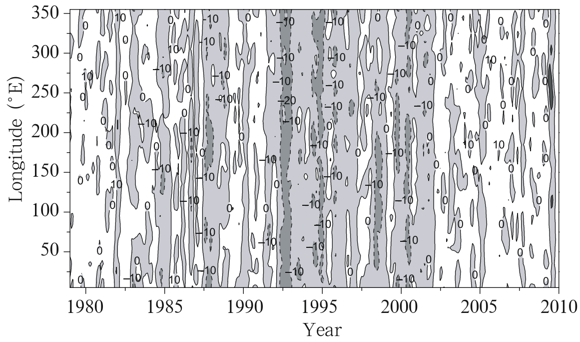

Fig. 9. Longitudinal distribution of ozone residuals obtained from Eq. (1) during 1979–2010. The solid and dashed lines denote positive and negative values, respectively. The absolute values larger than 10 DU are shaded.

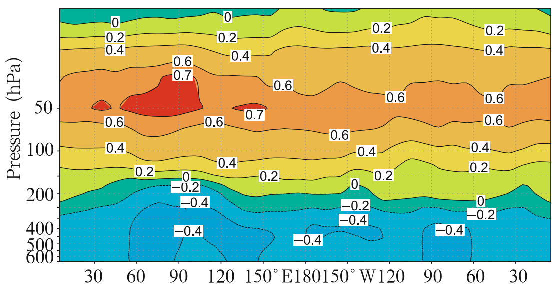

Fig. 10. Longitude-height cross-section of correlation coefficient between the total ozone and temperature over the Tibetan latitudes belt during 1979–2010.

tropopause around 100–200 hPa. The strong correlation between the total ozone and temperature has been found in previous studies (e.g., Newman and Randel, 1988; Randel and Cobb, 1994) and the correlation pattern is consistent with that of Ziemke et al. (1997). It should be noted that temperature is not the only parameter for this large contribution to the long-term ozone variation over the TP. As mentioned above, some other dynamical proxies, such as geopotential height and wind speed, could have similar contributions to the ozone variation over the TP. For example, strong negative correlation coefficients occur near the tropopause (around 100–200 hPa) between the total ozone and geopotential height (figure omitted). Applying temperature to the long-term ozone variation in Eq. (1) and the ozone residuals are obtained and shown in Fig. 11. It is clearly seen that the large difference between the observed ozone and

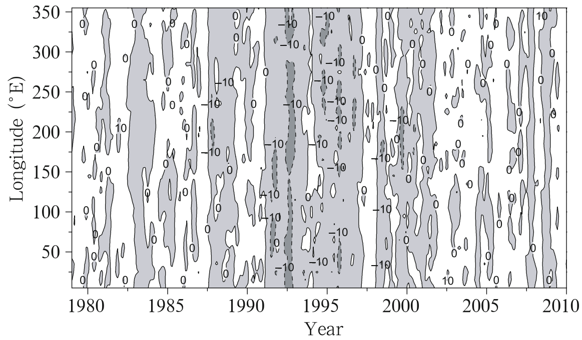

Fig. 11. Ozone anomaly (solid curve) and 50-hPa temperature-associated regression fit (dashed curve) from 1979 to 2010 over the (a) Tibetan and (b) non-Tibetan region.

regression fit becomes much smaller over the whole period of 1979–2010. The temperature contribution to the long-term ozone variation is also presented in Fig. 12a over the Tibetan region and in Fig. 12b over the non-Tibetan region. Over the Tibetan region, the temperature-associated regression fit indicates a 10% contribution to the total ozone, same as that of the QBO-associated regression fit. In particular, the lower temperature in those extremely low-ozone years contributes greatly to the ozone anomaly and reduces the residuals. Over the non-Tibetan region, however, the temperature-associated regression fit contributes only 4% of the total ozone variation, which is much smaller than that from the QBO-association regression fit. The larger impact of temperature on the long-term ozone variation over the Tibetan region than that over the non-Tibetan region is also consistent with the higher correlation coefficient over the Tibetan region in Fig. 10.

5. Summary and discussion

With the most recent merged TOMS/SBUV ozone data from 1979–2010, the variation and trend of the Tibetan ozone low were recalculated. Our results show that the Tibetan ozone low still exists during 1979–2010, with the severe ozone deficiency occurring in May and a monthly mean value of more than 35 DU lower than the zonal mean. Contrary to the global ozone recovery in the beginning of the 21st century, the Tibetan ozone deficiency may become a little

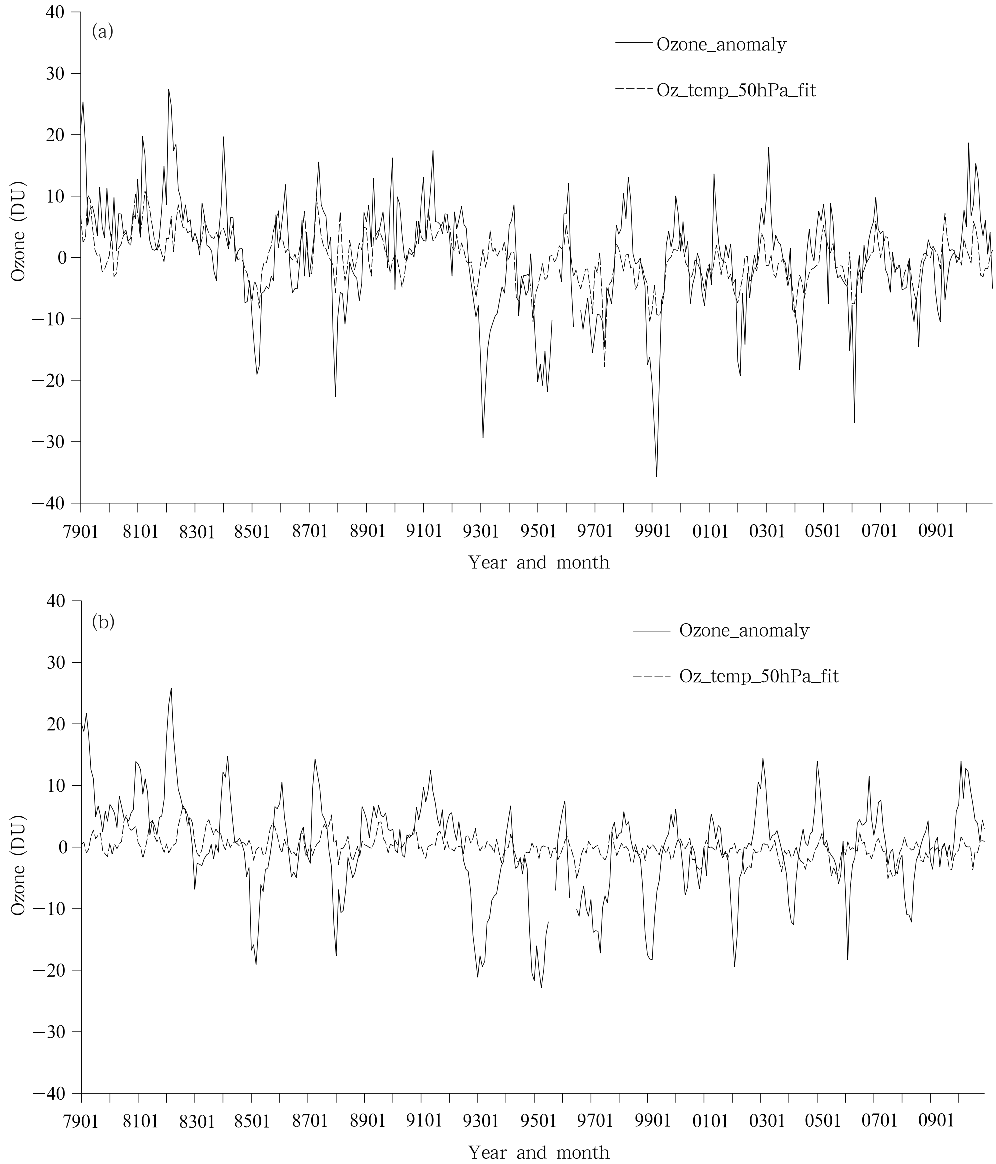

Fig. 12. As in Fig. 11, but with the 50-hPa temperature excluded in Eq. (1).

more strengthened during 2000–2010 than before 2000. Applying a standard statistical regression model to the total ozone, the long-term ozone variation and its possible affecting factors over the Tibetan latitudes belt are analyzed. The strong downward ozone trends occur in the winter-spring seasons, with the maximum value of –0.40±0.10 DU yr^{-1} in January over the Tibetan region and –0.29±0.09 DU yr^{-1} in February over the non-Tibetan region. Compared with the total ozone over the non-Tibetan region, the total ozone over the Tibetan region has a stronger downward trend during 1979–1999 and a weaker increasing trend during 2000–2010, which causes the larger average downward trends during 1979–2010 and the larger local ozone deficiency. Among the climate factors, the QBO signal greatly contributes to the long-term ozone variation over the whole Tibetan latitudes belt, accounting 10% and 9% of the total ozone variation over the Tibetan and non-Tibetan regions, respectively. Further analyses suggest that the local thermal-dynamical proxies, such as temperature and geopotential height have larger influences on the long-term ozone variation over the Tibetan than over the non-Tibetan region, which could be related to the local heating from the Tibetan Plateau. This study provides insight on the deepening of the severe ozone low over the Tibetan region under the background of global ozone recovery and the possible influencing climate factors for the long-term Tibetan ozone variation.

REFERENCES

Austin, J., K. Tourpali, E. Rozanov, et al., 2008: Coupled chemistry climate model simulations of the solar cycle in ozone and temperature. *J. Geophys. Res.*, **113**, D11306, doi: 10.1029/2007JD009391.

Baldwin, M. P., L. J. Gray, T. J. Dunkerton, et al., 2001: The quasi-biennial oscillation. *Rev. Geophys.*, **39**, 179–229.

Bian Jianchun, Li Weiliang, and Zhou Xiuji, 1997: Analysis of the seasonal variation feature of the wind structure over the Tibetan Plateau and its surroundings. *Ozone Changes Over China and Its Influences on Climate and Environment.* Zhou Xiuji, Ed., China Meteorological Press, Beijing, 257–273.

Bodeker, G. E., J. C. Scott, K. Kreher, et al., 2001: Global ozone trends in potential vorticity coordinates using TOMS and GOME intercompared against the Dobson network: 1978–1998. *J. Geophys. Res.*, **106**, 23029–23042.

Cong Chunhua, Li Weiliang, and Zhou Xiuji, 2001: The air mass exchange between the upper troposphere and lower stratosphere over the Tibetan Plateau and its surroundings. *Chinese Sci. Bull.*, **46**(22), 1914–1918. (in Chinese)

Farman, J. C., B. G. Gardiner, and J. D. Shanklin, 1985: Large losses of total ozone in Antarctica reveal seasonal ClOx/NOx interaction. *Nature*, **315**, 207–210, doi: 10.1038/315207a0.

Fioletov, V. E., G. E. Bodeker, A. J. Miller, et al., 2002: Global and zonal total ozone variations estimated from ground-based and satellite measurements. *J. Geophys. Res.*, **107**(D22), 4647, doi: 10.1029/2001JD001350.

Fu Chao, Li Weiliang, and Zhou Xiuji, 1997: Numerical simulation of the formation of ozone valley over the Tibetan Plateau and its surroundings. *Ozone Changes Over China and Its Influences on Climate and Environment.* Zhou Xiuji, Ed., China Meteorological Press, Beijing, 274–285.

Guillas, S., M. L. Stein, D. J. Wuebbles, et al., 2004: Using chemistry transport modeling in statistical analysis of stratospheric ozone trends from observations. *J. Geophys. Res.*, **109**, D22303, doi: 10.1029/2004JD005049.

Guo Dong, Wang Panxing, Zhou Xiuji, et al., 2012: Dynamic effects of the South Asian high on the ozone valley over the Tibetan Plateau. *Acta Meteor. Sinica*, **26**(2), 216–228, doi: 10.1007/s13351-012-0207-2.

Liu Yu and Li Weiliang, 2001: Deepening of ozone valley over the Tibetan Plateau and its possible influences. *Acta Meteor. Sinica*, **59**, 97–106. (in Chinese)

——, Li Weiliang, Zhou Xiuji, et al., 2003: Mechanism of formation of the ozone valley over the Tibetan Plateau in summer—Transport and chemical process of ozone. *Adv. Atmos. Sci.*, **20**(1), 103–109.

Manney, G. L., L. Froidevaux, J. W. Waters, et al., 1994: Chemical depletion of ozone in the Arctic lower stratosphere during winter 1992–93. *Nature*, **370**, 429–434.

Newchurch, M. J., E. -S. Yang, D. M. Cunnold, et al., 2003: Evidence for slowdown in stratospheric ozone loss: First stage of ozone recovery. *J. Geophys. Res.*, **108**, 4507, doi: 10.1029/2003JD003471.

Newman, P. A., and W. J. Randel, 1988: Coherent ozone-dynamical changes during the Southern Hemisphere spring, 1979–1986. *J. Geophys. Res.*, **93**, 12585–12606.

Randel, W. J., and J. B. Cobb, 1994: Coherent variations of monthly total ozone and lower stratosphereic temperature. *J. Geophys. Res.*, **99**, 5433–5447.

——, F. Wu, J. M. Russell III, et al., 1995: Ozone and temperature changes in the stratosphere following the eruption of Mount Pinatubo. *J. Geophys. Res.*, **100**, 16753–16764.

——, and M. Park, 2006: Deep convective influence on the Asian summer monsoon anticyclone and associated tracer variability observed with Atmospheric Infrared Sounder (AIRS). *J. Geophys. Res.*, **111**, D12314, doi: 10.1029/2005JD006490.

Reinsel, G. C., E. C. Weatherhead, G. C. Tiao, et al., 2002: On detection of turnaround and recovery in trend for ozone. *J. Geophys. Res.*, **107**, 4078, doi: 10.1029/2001JD000500.

——, A. J. Miller, E. C. Weatherhead, et al., 2005: Trend analysis of total ozone data for turnaround and dynamical contributions. *J. Geophys. Res.*, **110**, D16306, doi: 10.1029/2004JD004662.

Tian, W. S., M. Chipperfield, and Q. Huang, 2008: Effects of the Tibetan Plateau on total column ozone distribution. *Tellus*, **60B**, 622–635.

World Meteorological Organization (WMO), 2003: Scientific Assessment of Ozone Depletion: 2002. Global Ozone Research and Monitoring Project Report No. 47, Geneva, Switzerland, 498 pp.

——, 2007: Scientific Assessment of Ozone Depletion: 2006. Global Ozone Research and Monitoring Project Report No. 50, Geneva, Switzerland, 572 pp.

Xu Xiangde and Chen Lianshou, 2006: Advances of the study on Tibetan Plateau experiment of atmospheric sciences. *J. Appl. Meteor. Sci.*, **17**(6), 756–772.

Ye Zhuojia and Xu Yongfu, 2003: Climate characteristics of ozone over the Tibetan Plateau. *J. Geophys. Res.*, **108**(D20), 4654, doi: 10.1029/2002JD003139.

Zheng Xiangdong, Tang Jie, Li Weiliang, et al., 2000: Observational study on total ozone amount and its vertical profile over Lhasa in the summer of 1998. *J. Appl. Meteor. Sci.*, **11**, 173–179. (in Chinese)

Zhou, L. B., H. Akiyoshi, and K. Kawahira, 2003: Analysis of year-to-year ozone variation over the subtropical western Pacific region using EP_TOMS data and CCSR/NIES nudging CTM. *J. Geophys. Res.*, **108**, 4627, doi: 10.1029/2003 JD003412.

Zhou Shunwu and Zhang Renhe, 2005: Decadal variations of temperature and geopotential height over the Tibetan Plateau and their relations with Tibetan ozone depletion. *Geophys. Res. Lett.*, **32**, L18705.

Zhou Xiuji and Luo Chao, 1994: Ozone valley over the Tibetan Plateau, *Acta. Meteror. Sinica*, **8**, 505–506.

——, ——, Li Weiliang, et al., 1995: Variation of total ozone over China and the Tibetan Plateau low center. *Chinese Sci. Bull.*, **40**(15), 1396–1398. (in Chinese)

Ziemke, J. R., S. Chandra, R. D. McPeters, et al., 1997: Dynamical proxies of column ozone with applications to global trend models. *J. Geophys. Res.*, **102**, 6117–6129.

Zou Han, 1996: Seasonal variation and trends of TOMS ozone over Tibet. *Geophys. Res. Lett.*, **23**, 1029–1032.

—— and Gao Yongqi, 1997: Vertical ozone profile over Tibet using Sage I and II data. *Adv. Atmos. Sci.*, **14**, 505–512.

——, Ji Chongping, and Zhou Libo, 2000: QBO signal in total ozone over Tibet. *Adv. Atmos. Sci.*, **17**, 562–568.

——, ——, ——, et al., 2001: ENSO signal in total ozone over Tibet. *Adv. Atmos. Sci.*, **18**, 231–238.